Pnicogen-Bonded Anionic Complexes

ARTICLE *in* THE JOURNAL OF PHYSICAL CHEMISTRY A · APRIL 2014

Impact Factor: 2.69 · DOI: 10.1021/jp502667k · Source: PubMed

3 AUTHORS, INCLUDING:

Ibon Alkorta
Spanish National Research Council
680 PUBLICATIONS **12,430** CITATIONS
SEE PROFILE

José Elguero
Spanish National Research Council
1,502 PUBLICATIONS **22,206** CITATIONS
SEE PROFILE

THE JOURNAL OF PHYSICAL CHEMISTRY A

Article

pubs.acs.org/JPCA

Pnicogen-Bonded Anionic Complexes

Janet E. Del Bene,*[,†] Ibon Alkorta,*[,‡] and José Elguero[‡]

[†]Department of Chemistry, Youngstown State University, Youngstown, Ohio 44555, United States

[‡]Instituto de Química Médica (IQM−CSIC), Juan de la Cierva, 3, E-28006 Madrid, Spain

Supporting Information

ABSTRACT: Ab initio MP2/aug′-cc-pVTZ calculations have been carried out to investigate the pnicogen-bonded complexes $H_2YP{:}X^-$, for X,Y = Cl, NC, F, CCH, and CH_3. Of the 36 possible complexes, only 21 are unique equilibrium structures. All substituents form $(H_2XPX)^-$ complexes with symmetric X−P−X bonds. The P−A ion−molecule pnicogen bonds in these and some additional complexes have partial covalent character, while some P−A′ covalent bonds have partial ion−molecule character. A and A′ are the atoms of X and Y, respectively, which are directly bonded to P. Complexes with these types of bonds include the symmetric complexes $(H_2XPX)^-$, $H_2(CH_3)P{:}F^-$, $H_2(CCH)P{:}F^-$, $H_2FP{:}NC^-$, $H_2FP{:}Cl^-$, $H_2FP{:}CN^-$, and $H_2(NC)P{:}Cl^-$. Charge transfer from A to the P−A′ σ^* orbital stabilizes $H_2YP{:}X^-$ complexes and leads to a reduction of the negative charge on X. For fixed X, the smallest negative charge occurs in the symmetric complex. Then, for a given X, the order of decreasing negative charge with respect to Y is CH_3 > CCH > CN (bonded through C) > F > NC (bonded through N) > Cl, which is also the order of decreasing P−A distance. EOM-CCSD spin−spin coupling constants ^{1p}J(P−A) differentiate between shorter ion−molecule pnicogen bonds with partial covalent character and longer P···A ion−molecule pnicogen bonds. Similarly, coupling constants ^1J(P−A′) differentiate between longer covalent P−A′ bonds with partial ion−molecule character and shorter P−A′ covalent bonds.

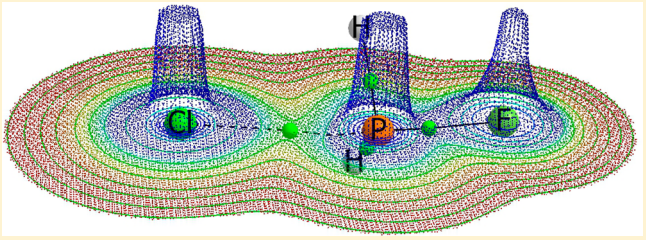

INTRODUCTION

The pnicogen (pnictogen) bond is a Lewis acid−Lewis base interaction in which a pnicogen atom such as P acts as the electron-pair acceptor. Previous studies of pnicogen bonds have identified many factors which influence the structures, energies, and other properties of the resulting complexes. These factors include the nature of the pnicogen atom,[1] the nature of the electron-donor base, substituent effects on the acid and the base,[2−11] and the formation of other intermolecular bonds by the pnicogen-bonded complex.[12−18] What is somewhat surprising is that there have been no investigations of complexes in which the base is an anion, except for a recent article which compared geometries and energies computed using different DFT functionals with the results of CCSD(T) calculations.[19] The subject of the present study is anionic pnicogen-bonded complexes.

In this article, we present the pnicogen-bonded complexes $H_2YP{:}X^-$, for X,Y = Cl, NC, F, CCH, and CH_3. We discuss the structures and binding energies of these complexes, their bonding properties and charge-transfer energies, and the spin−spin coupling constants ^{1p}J(P−A) and ^1J(P−A′), with A and A′ being the atoms of X and Y, respectively, which are directly bonded to P. We also discuss the degree of ion−molecule and covalent character of P−A and P−A′ bonds, and relate the bonding characteristics to other properties of these complexes, including spin−spin coupling constants. In addition, we provide a set of rules to determine for a given X,Y pair which substituent forms the covalent P−Y bond and which forms the P···X pnicogen bond.

METHODS

The structures of the monomers and the complexes $H_2YP{:}X^-$ were optimized at second-order Møller−Plesset perturbation theory (MP2)[20−23] with the aug′-cc-pVTZ basis set,[24] which is the Dunning aug-cc-pVTZ basis[25,26] with diffuse functions removed from H atoms. Frequencies were computed to ensure that the structures are equilibrium structures. The MP2 calculations were performed using the Gaussian 09 program.[27]

The Natural Bond Orbital (NBO) method[28] has been used to analyze the stabilizing charge-transfer interactions using the NBO-6 program.[29] Since MP2 orbitals are nonexistent, the charge-transfer energies were evaluated from B3LYP calculations[30,31] with the aug′-cc-pVTZ basis set at the MP2/aug′-cc-pVTZ geometries, so that at least some electron correlation effects would be included. NBO orbitals have been represented with the Jmol program[32] using the tools developed by Marcel Patek.[33] NBO electron populations have also been computed at MP2/aug′-cc-pVTZ.

Coupling constants were evaluated using the equation-of-motion coupled cluster singles and doubles (EOM-CCSD) method in the configuration interaction (CI)-like approximation[34,35] with all electrons correlated. For these calculations, the Ahlrichs[36] qzp basis set was placed on ^{13}C, ^{15}N, ^{17}O, and ^{19}F, and the qz2p basis set on ^{31}P and ^{35}Cl. The Dunning cc-pVDZ

Received: March 17, 2014
Revised: April 8, 2014
Published: April 24, 2014

Table 1. Binding Energies (kJ·mol^{-1}) of Complexes $H_2YP{:}X^-$[a]

$H_2YP{:}X^-$	$H_2(CH_3)P$	$H_2(CCH)P$	H_2FP	$H_2(CN)P$	$H_2(NC)P$	H_2ClP
X = CH_3	−70.0					
CCH	−24.0	−73.1				
F	−57.4	−119.8	−180.5			
CN	−17.7	−50.0	−126.5	−102.2		
NC	−19.8	−50.3	−98.5	−93.6	−131.8	
Cl	−19.4	−50.2	−85.4	−93.8	−120.9	−113.1

[a]Binding energies relative to the more stable monomers H_2YP + X^-.

basis set has been placed on ^{1}H atoms. All of the Ramsey terms, namely, the paramagnetic spin orbit (PSO), diamagnetic spin orbit (DSO), Fermi contact (FC), and spin dipole (SD), have been evaluated. The EOM-CCSD calculations were performed using ACES II[37] on the IBM Cluster 1350 (Glenn) at the Ohio Supercomputer Center.

RESULTS AND DISCUSSION

Structures and Binding Energies. With 6 substituents for X and Y, there are 36 possible complexes, but only 21 of these are unique equilibrium structures $H_2YP{:}X^-$. Table S1 of the Supporting Information provides the structures of these complexes, their molecular graphs, and total energies. These complexes may in principle have two different dissociation products, H_2YP and X^-, or Y^- and H_2XP. Table 1 lists the $H_2YP{:}X^-$ binding energies, which are defined as the negative of the dissociation energies relative to the more stable H_2YP and X^- products. The dissociation energies relative to Y^- and H_2XP are given in Table S2 of the Supporting Information. The diagonal elements of Table 1 are the energies of the complexes $(H_2XPX)^-$ that have C_{2v} symmetry and symmetric X−P−X bonds. When X and Y are different substituents, Table 1 allows the formulation of rules to determine which substituent is bonded as the anion X^- and which is the covalently bonded substituent Y.

1. If CH_3 is present, the complex is $H_2(CH_3)P{:}X^-$.
2. Omitting CH_3, if CCH is present, the complex is $H_2(CCH)P{:}X^-$.
3. Omitting CH_3 and CCH, if F is present, the complex is $H_2FP{:}X^-$.
4. Omitting CH_3, CCH, and F, if CN bonds through C, the complex is $H_2(CN)P{:}X^-$.
5. If Cl is present, it is the anion, and the complex is $H_2YP{:}Cl^-$.

These rules also include complexes containing NC with N bonded to P. Specifically, NC will be the anion NC^- except if Cl^- is present. Note that these rules reflect the ability of X to accommodate a negative charge, which is

$$Cl > NC > F > CCH > CH_3$$

It is also important to note that the binding energies of the symmetric complexes with X−P−X bonds decrease in the order

$$F \gg NC\ (\text{bonded at N}) > Cl > CN\ (\text{bonded at C}) > CCH \approx CH_3$$

which is not the same as the order based on the ability to accommodate a negative charge. That ability is the electron affinity of X, whereas the order of binding energies is related to the electronegativity of X. The complexes $H_2(CH_3)P{:}F^-$ and $(H_2FPF)^-$ are shown in Figure 1.

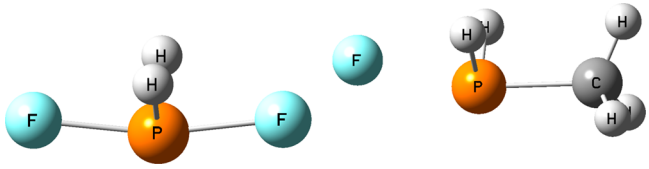

Figure 1. Symmetric molecular anion $(H_2FPF)^-$ and the anionic complex $H_2(CH_3)P{:}F^-$.

Before discussing the binding energies further, it is advantageous to first examine the structures of complexes $H_2YP{:}X^-$ that have C_s symmetry. These complexes can be described in terms of the P−A and P−A′ distances and the A−P−A′ angle, where A and A′ are the atoms of X and Y, respectively, which are directly bonded to P. In pnicogen-bonded complexes, the A−P−A′ arrangement tends toward linearity, with the A−P−A′ angle approaching 180°. For complexes $H_2YP{:}X^-$, this angle is consistent with the angles describing pnicogen bonds, varying between 162° and 169°, except for the complexes of $H_2(CH_3)P$ with CN^-, NC^-, and Cl^-, which have A−P−A′ angles between 152° and 156°.

Table 2 gives the P−A distances in complexes $H_2YP{:}X^-$. The P−A bonds in the symmetric anionic complexes $(H_2XPX)^-$ are relatively short and have some covalent character. To judge whether other P−A bonds have some degree of covalency, we have made the following assumption. If the P−A bond length in a complex $H_2YP{:}X^-$ is shorter than the P−A bond length in the corresponding symmetric structure, it has increased covalency relative to the bond in the symmetric complex. Moreover, if the P−A bond is longer than but within 0.30 Å of the length of the P−A bond in the symmetric structure, it still has some covalent character. Using these criteria, the two P−F bonds in $H_2(CH_3)P{:}F^-$ and $H_2(CCH)P{:}F^-$, the P−C bond in $H_2FP{:}CN^-$, the P−N bond in $H_2FP{:}NC^-$, and the P−Cl bonds in $H_2FP{:}Cl^-$ and $H_2(NC)P{:}Cl^-$ are ion−molecule pnicogen bonds with some degree of covalency.

Table S3 of the Supporting Information presents the values of the P−A′ distances. While the P−A′ bonds are shorter than the corresponding P−A bonds in the symmetric complexes, some of these bonds are long enough to suggest that they should be considered as P−A′ covalent bonds which have lost some degree of covalency and gained some ion−molecule character. The assumption is that if a P−A′ bond is within 0.15 Å of the length of the P−A bond in the corresponding symmetric complex, the P−A′ bond has a reduced degree of covalency relative to other corresponding P−A′ bonds and thus has some ion−molecule character. From Table S3, Supporting Information, these are the P−C bonds in $H_2(CH_3)P{:}F^-$ and $H_2(CCH)P{:}F^-$, the P−F bonds in $H_2FP{:}CN^-$, $H_2FP{:}NC^-$, and $H_2FP{:}Cl^-$, and the P−N bond in $H_2(NC)P{:}Cl^-$. These six complexes are the same six identified as having P−A ion−molecule pnicogen bonds with some covalent character.

dx.doi.org/10.1021/jp502667k | J. Phys. Chem. A 2014, 118, 3386−3392

Table 2. P−A Distances (Å) in Complexes $H_2YP{:}X^{-}$[a,b]

$H_2YP{:}X^-$	$H_2(CH_3)P$	$H_2(CCH)P$	H_2FP	$H_2(CN)P$	$H_2(NC)P$	H_2ClP
$X = CH_3$	*2.063*					
CCH	2.876	*2.079*				
F	*2.052*	*1.915*	*1.837*			
CN	3.115	2.662	*2.021*	*2.095*		
NC	2.975	2.614	*2.131*	2.357	*2.005*	
Cl	3.302	2.942	*2.595*	2.722	*2.475*	*2.388*

[a]A is the atom of X directly bonded to P. [b]Pnicogen P−A bonds with some covalent character are in italics.

Are the binding energies of the $H_2YP{:}X^-$ complexes related to the nature of the P−A and P−A′ bonds? From Table 1 it can be seen that for a fixed H_2YP, as the ability of X to accommodate a negative charge increases down a column, the binding energies decrease or are similar with two exceptions, $H_2(CH_3)P{:}F^-$ and $H_2(CCH)P{:}F^-$. These two complexes have significantly greater binding energies than the complexes directly above them. In addition, for a given substituent X^-, the binding energies of the complexes $H_2YP{:}X^-$ tend to increase from left to right across the row to the symmetric complex. There are three exceptions: $H_2FP{:}CN^-$, $H_2FP{:}NC^-$, and $H_2(NC)P{:}Cl^-$. The binding energies of these three complexes are greater than the binding energies of the complexes to their immediate right. These five complexes are five of the six complexes identified as having P−A bonds with partial covalent character and P−A′ bonds with partial ion−molecule character. Thus, the energies of these complexes reflect the degree of ion−molecule and covalent character of P−A and P−A′ bonds.

In complexes $H_2YP{:}Cl^-$, the order of decreasing P−Cl distance as a function of Y is

$$CH_3 > CCH > CN\ (\text{bonded at C}) > F > NC\ (\text{bonded at N}) > Cl$$

This order is common to all $H_2YP{:}X^-$ complexes for fixed X as a function of Y. Figure 2 provides a plot of the binding energies of $H_2YP{:}Cl^-$ complexes versus the P−Cl distance, illustrating a linear relationship between these two variables, with a correlation coefficient R^2 of 0.936. Plots of the binding energies of complexes $H_2YP{:}NC^-$, $H_2YP{:}CN^-$, and $H_2YP{:}F^-$ versus the P−A distances also show linear relationships with correlation coefficients R^2 of 0.958, 0.971, and 0.977, respectively.

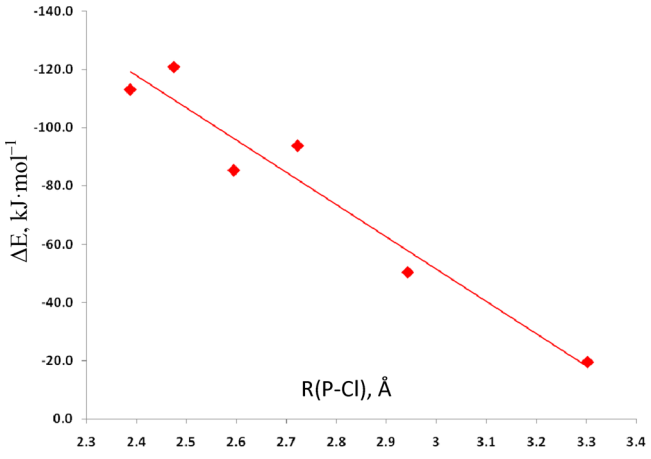

Figure 2. Binding energies of complexes $H_2YP{:}Cl^-$ versus the P−Cl distance as a function of Y.

NBO and AIM Analyses. Charge transfer occurs from a lone pair on A to the P−A′ σ^* orbital of H_2YP, as illustrated in Figure 3. The stabilizing charge-transfer energies are reported in Table 3. No entries are reported for the symmetric complexes $(H_2XPX)^-$ or $H_2FP{:}NC^-$ and $H_2FP{:}Cl^-$, since the NBO program considers these as single molecular ions. No charge-transfer data are reported for $H_2FP{:}CN^-$ since this complex is described by the program as $H_2(CN)P{:}F^-$. Complexes $H_2(CH_3)P{:}X^-$ and $H_2(CCH)P{:}X^-$ have the largest charge-transfer energies when X^- is F^-. For a given X^-, the charge-transfer energies increase across the row from left to right as the P−A bond length decreases, which suggests that charge transfer is more effective at shorter distances. Figure 4 shows the correlation between the charge-transfer energies and the P−Cl distance for $H_2YP{:}Cl^-$, with a correlation coefficient R^2 of 0.992.

Since charge transfer occurs from X^- to H_2YP, it is expected that the charge on X will be less than −1 au, which is apparent from the data in Table 4. For fixed Y, the negative charge on X^- is always smallest in the complex $(H_2XPX)^-$ since the charge is symmetrically distributed across the molecular ion. Then, for fixed X, it decreases in the order with respect to Y

$$CH_3 > CCH > CN > F > NC > Cl$$

which is also the order of decreasing P−A distance. The charge on X in the symmetric complexes $(H_2XPX)^-$ decreases in the order

$$F = NC > Cl > CN \approx CCH > CH_3$$

The molecular graphs derived from the electron densities of the $H_2YP{:}X^-$ complexes which are illustrated in Table S1 of the Supporting Information, show the presence of bond critical points (BCPs) and associated bond paths for both P−A and P−A′ bonds. Tables S3 and S4, Supporting Information, report the electron densities at the BCPs (ρ_{BCP}), the Laplacians of these densities ($\nabla^2\rho_{BCP}$), and the energy densities (H_{BCP}) for P−A and P−A′ bonds, respectively. Exponential relationships are found between the electron densities at the BCPs of both P−A and P−A′ bonds and the corresponding P−A and P−A′ distances, a relationship observed in previous studies.[38−46]

The electron densities at bond critical points are also indicators of the nature of the P−A and P−A′ bonds. Thus, ρ_{BCP} values for the P−A bonds in the six symmetric complexes $(H_2XPX)^-$ and the P−A bonds in $H_2(CH_3)P{:}F^-$, $H_2(CCH)P{:}F^-$, $H_2FP{:}CN^-$, $H_2FP{:}NC^-$, $H_2FP{:}Cl^-$, and $H_2(NC)P{:}Cl^-$ have the largest electron densities of 0.044e or greater. The only other P−A bond in this range is the P−N bond in $H_2(CN)P{:}NC^-$, which has a BCP density of 0.045e. Moreover, for fixed Y, all P−A′ bonds in these same complexes have electron densities at the BCPs that are smaller than the P−A′ densities for the remaining complexes in the series. The six symmetric complexes $(H_2XPX)^-$ and the complexes $H_2(CH_3)$-

dx.doi.org/10.1021/jp502667k | J. Phys. Chem. A 2014, 118, 3386−3392

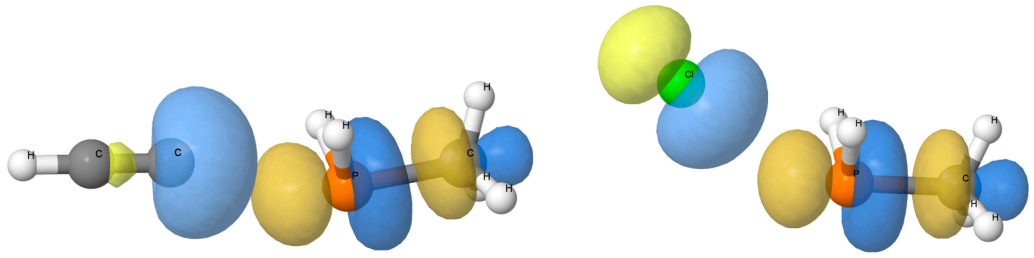

Figure 3. Lone pair orbitals of C in CCH^- and Cl^- and the σ^* P−C orbital of $H_2(CH_3)P$ involved in charge transfer interactions in $H_2(CH_3)P{:}CCH^-$ and $H_2(CH_3)P{:}Cl^-$.

Table 3. Charge-Transfer Stabilization Energies (kJ/mol) for Complexes $H_2YP{:}X^-$[a]

$H_2YP{:}X^-$	$H_2(CH_3)P$	$H_2(CCH)P$	H_2FP	$H_2(CN)P$	$H_2(NC)P$
X = CCH	46.4				
F	150.3	222.3			
CN	23.0	86.1	*b*		
NC	15.0	103.2	*c*	107.9	
Cl	16.3	49.4	*c*	96.2	230.2

[a]The NBO programs considers the $(H_2XPX)^-$ complexes as single molecular ions. [b]The NBO program considers this complex as $H_2(CN)P{:}F^-$. [c]The NBO program considers this complex as a single molecular ion.

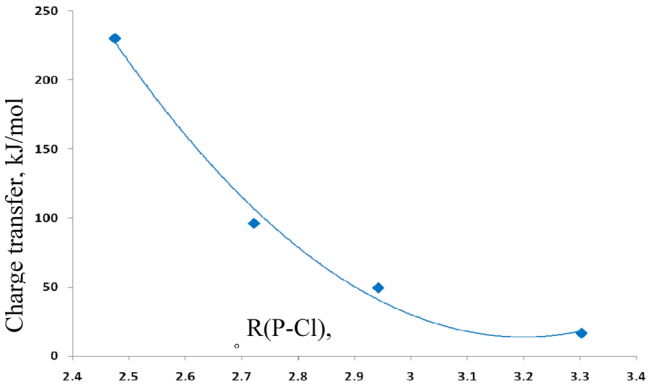

Figure 4. Charge-transfer energy versus the P−Cl distance for complexes $H_2YP{:}Cl^-$.

$P{:}F^-$, $H_2(CCH)P{:}F^-$, $H_2FP{:}CN^-$, $H_2FP{:}NC^-$, $H_2FP{:}Cl^-$, and $H_2(NC)P{:}Cl^-$ are those previously identified as having P−A bonds with reduced ion−molecule character and increased covalent character, and covalent P−A′ bonds with reduced covalency and increased ion−molecule character.

The Laplacians and the total energy densities have often been used to characterize bond types.[47−49] $\nabla^2\rho_{BCP}$ values are negative for the P−A bonds in $H_2FP{:}CN^-$ and in the symmetric $(H_2XPX)^-$ complexes with X = CH_3, CCH, CN, and NC. In addition, these same bonds and the P−A bonds in $(H_2FPF)^-$, $(H_2ClPCl)^-$, $H_2(CH_3)P{:}F^-$, $H_2(CCH)P{:}F^-$, $H_2FP{:}NC^-$, $H_2FP{:}Cl^-$, and $H_2(NC)P{:}Cl^-$ have H_{BCP} values that are also negative and greater in absolute value than 0.01 au, indicating that they have some covalent character. Moreover, in $H_2YP{:}X^-$ complexes for fixed Y, P−A′ bonds in these same complexes have less negative H_{BCP} values than the other P−A′ bonds in the same series, indicating that the former bonds have lost some covalency. Thus, the properties of the electron densities at bond critical points of P−A and P−A′ bonds are consistent with the characterization of these bonds based on distances and energies.

Spin−Spin Coupling Constants. Tables S6 and S7 of the Supporting Information provide the components of ^{1p}J(P−A) and ^{1}J(P−A′), respectively. The Fermi contact terms are not good approximations of ^{1p}J(P−A) for complexes $H_2YP{:}Cl^-$, $H_2YP{:}F^-$, and the symmetric complex $[H_2(CH_3)P{:}CH_3]^-$. They are also not good approximations of ^{1}J(P−A′) for $H_2(CH_3)P{:}X^-$, $H_2FP{:}X^-$, and the symmetric complex $(H_2ClP{:}Cl)^-$. All coupling constants reported in Table 5 are total J values.

Coupling constants ^{1p}J(P−Cl) across the pnicogen bonds for complexes $H_2YP{:}Cl^-$ are reported in Table 5, and the P−Cl distances are given in Table 2. The symmetric structure $(H_2ClP{:}Cl)^-$ has the shortest P−Cl distance, followed by the P−Cl distances in $H_2(NC)P{:}Cl^-$ and $H_2FP{:}Cl^-$. These three complexes have P−Cl pnicogen bonds with some covalent character. As a result, the values of ^{1p}J(P−Cl) for these three complexes are similar, varying between 85 and 88 Hz, and are significantly greater than the values of 71, 52, and 21 Hz for $H_2(CN)P{:}Cl^-$, $H_2(CCH)P{:}Cl^-$, and $H_2(CH_3)P{:}Cl^-$, respectively. Figure 5 presents a plot of ^{1p}J(P−Cl) versus the P−Cl distance for these complexes and illustrates the very good correlation between these two variables. The linear relationship shown has a correlation coefficient R^2 of 0.961. A second-order curve gives a slightly better fit with a correlation coefficient of 0.979.

Coupling constants ^{1p}J(P−N) for complexes $H_2YP{:}NC^-$ once again differentiate between P···N pnicogen bonds with and without some covalent character. Symmetric $[H_2(NC)P{:}NC]^-$ has the shortest P−N distance, followed by the P−N

Table 4. NBO MP2/aug′-cc-pVTZ Charges (au) on the Anions X^- in Complexes $H_2YP{:}X^-$

$H_2YP{:}X^-$	$H_2(CH_3)P$	$H_2(CCH)P$	H_2FP	$H_2(CN)P$	$H_2(NC)P$	H_2ClP
X = CH_3	−0.520					
CCH	−0.917	−0.615				
F	−0.808	−0.764	−0.730			
CN	−0.958	−0.871	−0.733	−0.617		
NC	−0.978	−0.933	−0.802	−0.870	−0.730	
Cl	−0.963	−0.907	−0.782	−0.838	−0.708	−0.629

dx.doi.org/10.1021/jp502667k | J. Phys. Chem. A 2014, 118, 3386−3392

Table 5. Spin−Spin Coupling Constants ^{1p}J(P−A) and ^{1}J(P−A′) (Hz) for Complexes $H_2YP{:}X^-$

complex	^{1p}J(P−A)	complex	^{1}J(P−A′)
$H_2YP{:}Cl^-$	^{1p}J(P−Cl)	$H_2(CH_3)P{:}X^-$	^{1}J(P−C)
Y = CH_3	21.0	X = CH_3	−32.9
CCH	51.5	CCH	11.5
F	85.2	F	19.4
CN	70.6	CN	5.3
NC	88.3	NC	5.6
Cl	85.5	Cl	3.6
$H_2YP{:}NC^-$	^{1p}J(P−N)	$H_2(CCH)P{:}X^-$	^{1}J(P−C)
Y = CH_3	−26.0	X = CCH	−57.8
CCH	−43.4	F	−87.2
F	−3.8	CN	−46.5
CN	−36.2	NC	−38.0
NC	13.7	Cl	−41.5
$H_2YP{:}CN^-$	^{1p}J(P−C)	$H_2FP{:}X^-$	^{1}J(P−F)
Y = CH_3	73.3	X = F	164.1
CCH	99.1	CN	137.2
F	−81.0	NC	9.4
CN	−36.9	Cl	−100.8
$H_2YP{:}F^-$	^{1p}J(P−F)	$H_2(CN)P{:}X^-$	^{1}J(P−C)
Y = CH_3	273.7	X = CN	−36.9
CCH	230.4	NC	−62.5
F	164.1	Cl	−67.2
$H_2YP{:}CCH^-$	^{1p}J(P−C)	$H_2(NC)P{:}X^-$	^{1}J(P−N)
Y = CH_3	95.8	X = NC	13.7
CCH	−57.8	Cl	30.9
$H_2YP{:}CH_3^-$	^{1p}J(P−C)	$H_2ClP{:}X^-$	^{1}J(P−Cl)
Y = CH_3	−32.9	X = Cl	85.5

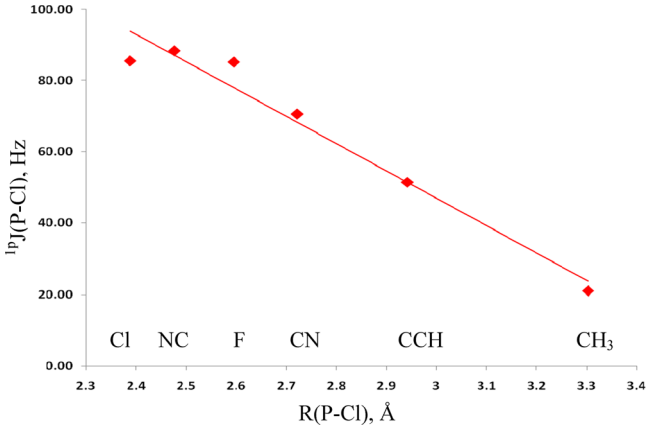

Figure 5. ^{1p}J(P−Cl) versus the P−Cl distance for complexes $H_2YP{:}Cl^-$. Points are identified at the bottom of the graph by the nature of Y.

distance in $H_2FP{:}NC^-$. These two complexes have ^{1p}J(P−N) values of 14 and −4 Hz, respectively, while the remaining three complexes have ^{1p}J(P−N) values between −26 and −43 Hz at significantly longer P−N distances. Similarly, the P−C distances in $[H_2(CN)P{:}CN]^-$ and $H_2FP{:}CN^-$ are 2.095 and 2.021 Å, the only case in which the P−A distance in the symmetric structure is not the shortest distance, and ^{1p}J(P−C) values for $H_2FP{:}CN^-$ and $[H_2(CN)P{:}CN]^-$ are −81 and −37 Hz, respectively. The remaining two complexes $H_2(CCH)P{:}CN^-$ and $H_2(CH_3)P{:}CN^-$ have ^{1p}J(P−C) values of 99 and 73 Hz at longer P−C distances. Thus, coupling constants can distinguish between P−A pnicogen bonds with increased covalent character and shorter bond lengths and P−A bonds that are essentially ion−molecule pnicogen bonds with longer P−A distances.

Do ^{1}J(P−A′) values differentiate between normal covalent bonds and those bonds with reduced covalency and increased ion−molecule character? Table 5 also presents the values of ^{1}J(P−A′), and Table S2, Supporting Information, gives the P−A′ distances. Since the P−A′ bonds are covalent bonds, the P−A′ distance in the symmetric structure is the longest P−A′ distance. The P−C distance in $[H_2(CH_3)P{:}CH_3]^-$ is 2.063 Å. Shorter P−C distances of 1.960 and 1.903 Å are found in $H_2(CH_3)P{:}F^-$ and $H_2(CH_3)P{:}CCH^-$, and the shortest distances of 1.88 Å are found in the remaining three complexes. Figure 6 presents a plot of ^{1}J(P−C) versus the P−C distance,

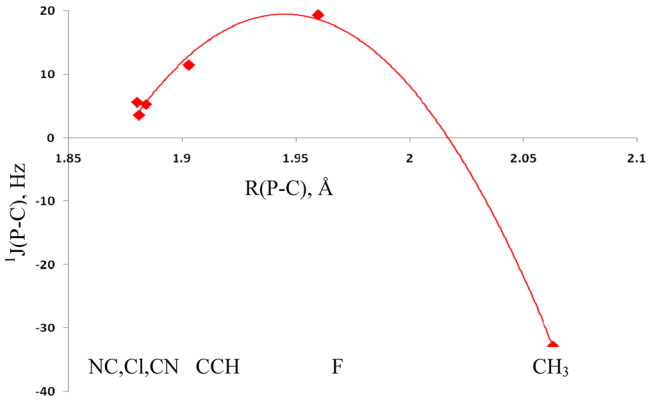

Figure 6. ^{1}J(P−C) versus the P−C distance for complexes $H_2(CH_3)P{:}X^-$. Points are identified at the bottom of the graph by the nature of X.

which dramatically illustrates the effect of the P−C bond losing some covalency and acquiring some ion−molecule character. ^{1}J(P−C) for $[H_2(CH_3)P{:}CH_3]^-$ is −33 Hz but then increases and exhibits its maximum value of approximately 19 Hz for $H_2(CH_3)P{:}F^-$. It then decreases to 11.5 Hz for $H_2(CH_3)P{:}CCH^-$ and decreases further to between 4 and 6 Hz for the remaining three complexes. The correlation coefficient for the second-order curve in Figure 6 is 0.996. The variation of ^{1}J(P−C) would be difficult to understand without some knowledge of the nature of the P−A′ bonds and their variation with distance.

^{1}J(P−C) as a function of the P−C distance for $H_2(CCH)P{:}X^-$ is illustrated in Figure 7 and shows a similar pattern.

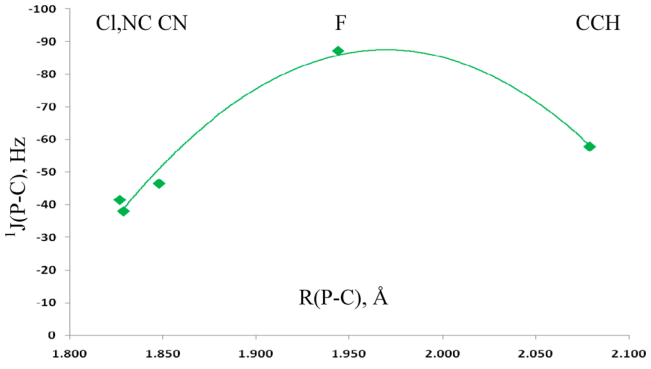

Figure 7. ^{1}J(P−C) versus the P−C distance for complexes $H_2(CCH)P{:}X^-$. Points are identified at the top of the graph by the nature of X.

dx.doi.org/10.1021/jp502667k | J. Phys. Chem. A 2014, 118, 3386−3392

$[H_2(CCH)P:CCH]^-$ has the longest P−C bond at 2.079 Å and a value of ^1J(P−C) of −58 Hz. As the P−C bond becomes shorter and the ion−molecule character decreases, ^{1}J(P−C) increases in absolute value and has its maximum value of −87 Hz for $H_2(CCH)P:F^-$. The remaining three complexes have covalent P−C bonds with short P−C distances and decreased absolute values of ^{1}J(P−C), which cluster between −38 and −47 Hz. The correlation coefficient for the trendline in Figure 7 is 0.974. The remaining complexes with Y = F, CN, and NC also have coupling constants which differentiate between P−A′ covalent bonds with some ion−molecule character and those that are essentially covalent bonds. Thus, the recognition of the partial ion−molecule character of the longer bonds is essential for understanding the values of ^1J(P−A′).

CONCLUSIONS

Ab initio MP2/aug′-cc-pVTZ calculations have been carried out to investigate the pnicogen-bonded complexes $H_2YP:X^-$, for X,Y = Cl, NC, F, CCH, and CH_3. The results of this study support the following statements.

1. Of the 36 possible complexes, only 21 unique equilibrium structures exist. A hierarchy has been established to determine which substituent is covalently bonded to P as Y, and which forms the P···X pnicogen bond. If CH_3 is present it is Y, then CCH, followed by F, then CN bonded through C, NC bonded through N, and finally Cl. This ordering is determined by the ability of X to accommodate a negative charge.
2. All substituents form complexes $(H_2XPX)^-$ with C_{2v} symmetry and symmetric X−P−X bonds. These complexes have ion−molecule P···A pnicogen bonds with some covalent character.
3. On the basis of the lengths of P−A and P−A′ bonds, with A the atom of X and A′ the atom of Y which are directly bonded to P, some complexes have P···A pnicogen bonds with reduced ion−molecule character and increased covalent character, and covalent P−A′ bonds with reduced covalent character and increased ion−molecule character.
4. The symmetric complexes and complexes with P−A pnicogen bonds with partial covalent character and P−A′ bonds with some ion−molecule character have relatively high binding energies. The latter complexes include $H_2(CH_3)P:F^-$, $H_2(CCH)P:F^-$, $H_2FP:NC^-$, $H_2FP:Cl^-$, $H_2FP:CN^-$, and $H_2(NC)P:Cl^-$.
5. Charge transfer from A to the P−A′ σ^* orbital stabilizes $H_2YP:X^-$ complexes and leads to a reduction of the negative charge on X. The smallest negative charges on X are found in the symmetric complexes. Then, for fixed X, the order of decreasing negative charge with respect to Y is CH_3 > CCH > CN (bonded through C) > F > NC (bonded through N) > Cl, which is the same as the order of decreasing P−A distance.
6. Spin−spin coupling constants ^{1p}J(P−A) differentiate between shorter ion−molecule pnicogen bonds with partial covalent character and longer P···A ion−molecule pnicogen bonds. Similarly, coupling constants ^1J(P−A′) differentiate between longer covalent P−A′ bonds with partial ion−molecule character and shorter P−A′ covalent bonds.

ASSOCIATED CONTENT

Supporting Information

Geometries, total energies, and molecular graphs for complexes $H_2YP:X^-$; binding energies of $H_2YP:X^-$ relative to $H_2YP + X^-$ and $H_2XP + Y^-$; P−A′ distances; properties of electron densities at P−A and P−A′ bond critical points; ^{1p}J(P−A) and ^1J(P−A′) and their components for complexes $H_2YP:X^-$; full refs 27 and 37. This material is available free of charge via the Internet at http://pubs.acs.org.

AUTHOR INFORMATION

Corresponding Authors

*(J.E.D.B.) E-mail: jedelbene@ysu.edu.
*(I.A.) E-mail: ibon@iqm.csic.es.

Notes

The authors declare no competing financial interest.

ACKNOWLEDGMENTS

This work was carried out with financial support from the Ministerio de Economía y Competitividad (Project No. CTQ2012-35513-C02-02) and Comunidad Autónoma de Madrid (Project MADRISOLAR2, ref S2009/PPQ1533). Thanks are also given to the Ohio Supercomputer Center and CTI (CSIC) for continued support.

REFERENCES

(1) Zahn, S.; Frank, R.; Hey-Hawkins, E.; Kirchner, B. Pnicogen Bonds: A New Molecular Linker? *Chem.—Eur. J.* **2011**, *17*, 6034−6038.
(2) Scheiner, S. Effects of Multiple Substitution upon the P···N Noncovalent Interaction. *Chem. Phys.* **2011**, *387*, 79−84.
(3) Adhikari, U.; Scheiner, S. Substituent Effects on Cl···N, S···N, and P···N Noncovalent Bonds. *J. Phys. Chem. A* **2012**, *116*, 3487−3497.
(4) Adhikari, U.; Scheiner, S. Effects of Carbon Chain Substituents on the P···N Noncovalent Bond. *Chem. Phys. Lett.* **2012**, *536*, 30−33.
(5) Del Bene, J. E.; Alkorta, I.; Sanchez-Sanz, G.; Elguero, J. $^{31}P-^{31}P$ Spin−Spin Coupling Constants for Pnicogen Homodimers. *Chem. Phys. Lett.* **2011**, *512*, 184−187.
(6) Del Bene, J. E.; Alkorta, I.; Sanchez-Sanz, G.; Elguero, J. Structures, Energies, Bonding, and NMR Properties of Pnicogen Complexes $H_2XP:NXH_2$ (X = H, CH_3, NH_2, OH, F, Cl). *J. Phys. Chem. A* **2011**, *115*, 13724−13731.
(7) Alkorta, I.; Elguero, J.; Del Bene, J. E. Pnicogen Bonded Complexes of PO_2X (X = F, Cl) with Nitrogen Bases. *J. Phys. Chem. A* **2013**, *117*, 10497−10503.
(8) Del Bene, J. E.; Alkorta, I.; Elguero, J. Characterizing Complexes with Pnicogen Bonds Involving sp^2 Hybridized Phosphorus Atoms: $(H_2C{=}PX)_2$ with X = F, Cl, OH, CN, NC, CCH, H, CH_3, and BH_2. *J. Phys. Chem. A* **2013**, *117*, 6893−6903.
(9) Del Bene, J. E.; Alkorta, I.; Elguero, J. Properties of Complexes $H_2C{=}(X)P:PXH_2$, for X = F, Cl, OH, CN, NC, CCH, H, CH_3, and BH_2: P···P Pnicogen Bonding at σ-Holes and π-Holes. *J. Phys. Chem. A* **2013**, *117*, 11592−11604.
(10) Alkorta, I.; Elguero, J.; Del Bene, J. E. Pnicogen-Bonded Cyclic Trimers $(PH_2X)_3$ with X = F, Cl, OH, NC, CN, CH_3, H, and BH_2. *J. Phys. Chem. A* **2013**, *117*, 4981−4987.
(11) Alkorta, I.; Sánchez-Sanz, G.; Elguero, J.; Del Bene, J. E. Exploring $(NH_2F)_2$, $H_2FP:NFH_2$, and $(PH_2F)_2$ Potential Surfaces: Hydrogen Bonds or Pnicogen Bonds? *J. Phys. Chem. A* **2013**, *117*, 183−191.
(12) Alkorta, I.; Sánchez-Sanz, G.; Elguero, J.; Del Bene, J. E. Influence of Hydrogen Bonds on the P···P Pnicogen Bond. *J. Chem. Theory Comput.* **2012**, *8*, 2320−2327.
(13) Del Bene, J. E.; Alkorta, I.; Sánchez-Sanz, G.; Elguero, J. Interplay of F−H···F Hydrogen Bonds and P···N Pnicogen Bonds. *J. Phys. Chem. A* **2012**, *116*, 9205−9213.

(14) Del Bene, J. E.; Alkorta, I.; Sánchez-Sanz, G.; Elguero, J. Phosphorus As a Simultaneous Electron-Pair Acceptor in Intermolecular P···N Pnicogen Bonds and Electron-Pair Donor to Lewis Acids. *J. Phys. Chem. A* **2013**, *117*, 3133−3141.
(15) Li, Q.-Z.; Li, R.; Liu, X.-F.; Li, W.-Z.; Cheng, J.-B. Concerted Interaction between Pnicogen and Halogen Bonds in XCl−FH_2P−NH_3 (X = F, OH, CN, NC, and FCC). *ChemPhysChem* **2012**, *13*, 1205−1212.
(16) An, X.-L.; Li, R.; Li, Q.-Z.; Liu, X.-F.; Li, W.-Z.; Cheng, J.-B. Substitution, Cooperative, and Solvent Effects on π Pnicogen Bonds in the FH_2P and FH_2As Complexes. *J. Mol. Model.* **2012**, *18*, 4325−4332.
(17) Li, Q.; Zhuo, H.; Yang, X.; Cheng, J.; Li, W.; Loffredo, R. E. Cooperative and Diminutive Effects of Pnicogen Bonds and Cation−π Interactions. *ChemPhysChem* **2014**, *15*, 500−506.
(18) Solimannejad, M.; Bayati, E.; Esrafili, M. D. Enhancement Effect of Lithium Bonding on the Strength of Pnicogen Bonds: XH_2P···NCLi···NCY as a Working Model (X = F, Cl; Y = H, F, Cl, CN). *Mol. Phys.* **2014**, DOI: 10.1080/00268976.2014.884250.
(19) Bauzá, A.; Alkorta, I.; Frontera, A.; Elguero, J. On the Reliability of Pure and Hybrid DFT Methods for the Evaluation of Halogen, Chalcogen, and Pnicogen Bonds Involving Anionic and Neutral Electron Donors. *J. Chem. Theory Comput.* **2013**, *9*, 5201−5210.
(20) Pople, J. A.; Binkley, J. S.; Seeger, R. Theoretical Models Incorporating Electron Correlation. *Int. J. Quantum Chem., Quantum Chem. Symp.* **1976**, *S10*, 1−19.
(21) Krishnan, R.; Pople, J. A. Approximate Fourth-Order Perturbation Theory of the Electron Correlation Energy. *Int. J. Quantum Chem.* **1978**, *14*, 91−100.
(22) Bartlett, R. J.; Silver, D. M. Many-Body Perturbation Theory Applied to Electron Pair Correlation Energies. I. Closed-Shell First-Row Diatomic Hydrides. *J. Chem. Phys.* **1975**, *62*, 3258−3268.
(23) Bartlett, R. J.; Purvis, G. D. Many-Body Perturbation Theory, Coupled-Pair Many-Electron Theory, and the Importance of Quadruple Excitations for the Correlation Problem. *Int. J. Quantum Chem.* **1978**, *14*, 561−581.
(24) Del Bene, J. E. Proton Affinities of Ammonia, Water, and Hydrogen Fluoride and Their Anions: a Quest for the Basis-Set Limit Using the Dunning Augmented Correlation-Consistent Basis Sets. *J. Phys. Chem.* **1993**, *97*, 107−110.
(25) Dunning, T. H. Gaussian Basis Sets for Use in Correlated Molecular Calculations. I. The Atoms Boron Through Neon and Hydrogen. *J. Chem. Phys.* **1989**, *90*, 1007−1023.
(26) Woon, D. E.; Dunning, T. H. Gaussian Basis Sets for Use in Correlated Molecular Calculations. V. Core−Valence Basis Sets for Boron Through Neon. *J. Chem. Phys.* **1995**, *103*, 4572−4585.
(27) Frisch, M. J.; Trucks, G. W.; Schlegel, H. B.; Scuseria, G. E.; Robb, M. A.; Cheeseman, J. R.; Scalmani, G.; Barone, V.; Mennucci, B.; Petersson, G. A.; et al. *Gaussian 09*; Gaussian, Inc.: Wallingford, CT, 2009.
(28) Reed, A. E.; Curtiss, L. A.; Weinhold, F. Intermolecular Interactions from a Natural Bond Orbital, Donor−Acceptor Viewpoint. *Chem. Rev.* **1988**, *88*, 899−926.
(29) Glendening, E. D.; Badenhoop, J. K.; Reed, A. E.; Carpenter, J. E.; Bohmann, J. A.; Morales, C. M.; Landis, C. R.; Weinhold, F. *NBO 6.0*; University of Wisconsin: Madison, WI, 2013.
(30) Becke, A. D. Density-Functional Thermochemistry. III. The Role of Exact Exchange. *J. Chem. Phys.* **1993**, *98*, 5648−5652.
(31) Lee, C.; Yang, W.; Parr, R. G. Development of the Colle−Salvetti Correlation-Energy Formula into a Functional of the Electron Density. *Phys. Rev. B* **1988**, *37*, 785−789.
(32) Jmol: an Open-Source Java Viewer for Chemical Structures in 3D, version 13.0. http://www.jmol.org/ (accessed on Sept 26th, 2013).
(33) Patek, M. Jmol NBO Visualization Helper program. http://www.marcelpatek.com/nbo/nbo.html (accessed on Sept 26th, 2013).
(34) Perera, S. A.; Nooijen, M.; Bartlett, R. J. Electron Correlation Effects on the Theoretical Calculation of Nuclear Magnetic Resonance Spin−Spin Coupling Constants. *J. Chem. Phys.* **1996**, *104*, 3290−3305.
(35) Perera, S. A.; Sekino, H.; Bartlett, R. J. Coupled-Cluster Calculations of Indirect Nuclear Coupling Constants: The Importance of non-Fermi Contact Contributions. *J. Chem. Phys.* **1994**, *101*, 2186−2191.
(36) Schäfer, A.; Horn, H.; Ahlrichs, R. Fully Optimized Contracted Gaussian Basis Sets for Atoms Li to Kr. *J. Chem. Phys.* **1992**, *97*, 2571−2577.
(37) Stanton, J. F.; Gauss, J.; Watts, J. D.; Nooijen, M.; Oliphant, N.; Perera, S. A.; Szalay, P. G.; Lauderdale, W. J.; Gwaltney, S. R.; Beck, S.; et al. *ACES II*, a program product of the Quantum Theorey Project; University of Florida: Gainesville, FL; Integral packages included are VMOL (J. Almlöf and Taylor PR); VPROPS (P. R. Taylor); and ABACUS (T Helgaker, H. J. Aa. Jensen, P. Jørgensen, J. Olsen, and P. R. Taylor). Brillouin-Wigner perturbation theory was implement by J. Pittner.
(38) Knop, O.; Boyd, R. J.; Choi, S. C. Sulfur−Sulfur Bond Lengths, or Can a Bond Length Be Estimated from a Single Parameter? *J. Am. Chem. Soc.* **1988**, *110*, 7299−7301.
(39) Gibbs, G. V.; Hill, F. C.; Boisen, M. B.; Downs, R. T. Power Law Relationships between Bond Length, Bond Strength and Electron Density Distributions. *Phys. Chem. Miner.* **1998**, *25*, 585−590.
(40) Alkorta, I.; Barrios, L.; Rozas, I.; Elguero, J. Comparison of Models to Correlate Electron Density at the Bond Critical Point and Bond Distance. *J. Mol. Struct.* **2000**, *496*, 131−137.
(41) Knop, O.; Rankin, K. N.; Boyd, R. J. Coming to Grips with N−H···N Bonds. 1. Distance Relationships and Electron Density at the Bond Critical Point. *J. Phys. Chem. A* **2001**, *105*, 6552−6566.
(42) Knop, O.; Rankin, K. N.; Boyd, R. J. Coming to Grips with N−H···N Bonds. 2. Homocorrelations between Parameters Deriving from the Electron Density at the Bond Critical Point. *J. Phys. Chem. A* **2003**, *107*, 272−284.
(43) Espinosa, E.; Alkorta, I.; Elguero, J.; Molins, E. From Weak to Strong Interactions: A Comprehensive Analysis of the Topological and Energetic Properties of the Electron Density Distribution Involving X−H···F−Y Systems. *J. Chem. Phys.* **2002**, *117*, 5529−5542.
(44) Alkorta, I.; Elguero, J. Fluorine−Fluorine Interactions: NMR and AIM Analysis. *Struct. Chem.* **2004**, *15*, 117−120.
(45) Tang, T. H.; Deretey, E.; Knak Jensen, S. J.; Csizmadia, I. G. Hydrogen Bonds: Relation Between Lengths and Electron Densities at Bond Critical Points. *Eur. Phys. J. D* **2006**, *37*, 217−222.
(46) Mata, I.; Alkorta, I.; Molins, E.; Espinosa, E. Universal Features of the Electron Density Distribution in Hydrogen-Bonding Regions: A Comprehensive Study Involving H···X (X = H, C, N, O, F, S, Cl, π) Interactions. *Chem.—Eur. J.* **2010**, *16*, 2442−2452.
(47) Cramer, P.; Kraka, E. A Description of the Chemical Bond in Terms of Local Properties of Electron Density and Energy. *Croat. Chem. Acta* **1984**, *57*, 1259−1281.
(48) Rozas, I.; Alkorta, I.; Elguero, J. The Behaviour of Ylides Containing N, O and C Atoms as Hydrogen Bond Acceptors. *J. Am. Chem. Soc.* **2000**, *122*, 11154−11161.
(49) Grabowski, S. J. Covalent Character of Hydrogen Bonds Enhanced by π-Electron Delocalization. *Croat. Chem. Acta* **2009**, *82*, 185−192.